Front. Phys. 11(2), 117102 (2016)
DOI 10.1007/s11467-015-0536-3

RESEARCH ARTICLE

Scaling behavior of the thermopower of the archetypal heavy-fermion metal $YbRh_2Si_2$

V. R. Shaginyan[1,2,†], A. Z. Msezane[2], G. S. Japaridze[2], K. G. Popov[3,4], J. W. Clark[5,6], V. A. Khodel[5,7]

[1] *Petersburg Nuclear Physics Institute, NRC Kurchatov Institute, Gatchina, 188300, Russia*
[2] *Clark Atlanta University, Atlanta, GA 30314, USA*
[3] *Komi Science Center, Ural Division, RAS, Syktyvkar, 167982, Russia*
[4] *Department of Physics, St. Petersburg State University, Russia*
[5] *McDonnell Center for the Space Sciences & Department of Physics, Washington University, St. Louis, MO 63130, USA*
[6] *Centro de Ciências Matemáticas, Universidade de Madeira, 9000-390 Funchal, Madeira, Portugal*
[7] *Russian Research Center Kurchatov Institute, Moscow, 123182, Russia*

Corresponding author. E-mail: [†] *vrshag@thd.pnpi.spb.ru*

Received October 13, 2015; accepted November 13, 2015

We reveal and explain the scaling behavior of the thermopower S/T exhibited by the archetypal heavy-fermion (HF) metal $YbRh_2Si_2$ under the application of magnetic field B at temperature T. We show that the same scaling is demonstrated by different HF compounds such as β-$YbAlB_4$ and the strongly correlated layered cobalt oxide $[BiBa_{0.66}K_{0.36}O_2]CoO_2$. Using $YbRh_2Si_2$ as an example, we demonstrate that the scaling behavior of S/T is violated at the antiferromagnetic phase transition, while both the residual resistivity ρ_0 and the density of states, N, experience jumps at the phase transition, causing the thermopower to make two jumps and change its sign. Our elucidation is based on flattening of the single-particle spectrum that profoundly affects ρ_0 and N. To depict the main features of the S/T behavior, we construct a T–B schematic phase diagram of $YbRh_2Si_2$. Our calculated S/T for the HF compounds are in good agreement with experimental facts and support our observations.

Keywords thermoelectric and thermomagnetic effects, quantum phase transition, flat bands, non-Fermi-liquid states, strongly correlated electron systems, heavy fermions

PACS numbers 71.27.+a, 72.15.Jf, 64.70.Tg

1 Introduction

It is ordinarily believed that the behavior of heavy-fermion (HF) metals is determined by the quantum critical point (QCP), which suppresses quasiparticle excitations and results in non-Fermi-liquid (NFL) behavior, revealing vivid deviations from Landau Fermi liquid (LFL) behavior; see, e.g., [1, 2]. The NFL behavior is commonly characterized by a set of exponents of the temperature dependence of the physical properties, such as specific heat, resistivity, and susceptibility [1–4]. The LFL and NFL behaviors and the crossover region cannot be captured by any single exponent, as seen, for example, from Fig. 1(a), which depicts the behavior of the normalized specific heat $(C/T)_N$ extracted from measurements of the specific heat $C/T \propto M^*$ on $YbRh_2Si_2$ under the application of magnetic fields B [5], where M^* is the effective mass and T is temperature. It is seen that the curves $(C/T)_N$ obtained in measurements at different magnetic fields B merge into a single one, exhibiting a scaling behavior [3, 4, 6]. This scaling behavior provides an adequate description within the framework of fermion condensation (FC) theory, which supports the extended quasiparticle paradigm [3, 4].

Thermopower S/T is a sensitive and helpful probe for disentangling the electronic excitations at the Fermi surface. Thus, we face an important problem related to the revelation of the scaling behavior of the thermopower S/T, which allows one to analyze the nature of electronic excitations at the Fermi surface. Along this line, we shall clarify the role of quasiparticles and flat bands and the nature of electronic excitations that form the behavior of the thermopower S/T in different HF compounds.

In this Rapid Communication, we demonstrate that the thermopower S/T of the archetypal HF metal $YbRh_2Si_2$ exhibits a scaling behavior that coincides with that of other thermodynamic functions such as the normalized specific heat $(C/T)_N$. We show that S/T of different HF compounds such as $YbRh_2Si_2$, β-$YbAlB_4$, and $[BiBa_{0.66}K_{0.36}O_2]CoO_2$ exhibits the same scaling behavior, coinciding with that of $(C/T)_N$ shown in Fig. 1(a). Using the archetypal HF metal $YbRh_2Si_2$ as an example, we also demonstrate that the universal behavior of S/T is violated at the antiferromagnetic (AF) phase transition, while the residual resistivity ρ_0 and the density of states, N, experience jumps at the phase transition. This results in corresponding downward jumps of S/T and its change of sign. To depict the main features of the S/T behavior, we construct a schematic T–B phase diagram. Our calculated S/T of $YbRh_2Si_2$, β-$YbAlB_4$, and $[BiBa_{0.66}K_{0.36}O_2]CoO_2$ are found to be in good agreement with experimental observations.

2 Scaling behavior

A study of the thermoelectric power S/T may deliver new insight into the nature of the quantum phase transition that defines the NFL behavior of the corresponding HF compound. For example, one may reasonably propose that the thermoelectric power S/T distinguishes between two competing scenarios for quantum phase transitions in heavy fermions, namely, spin-density-wave theory and the breakdown of the Kondo effect [7, 8]. Indeed, S/T is sensitive to the derivative of the density of electronic states and the change in the relaxation time at μ [9, 10]. Using the Boltzmann equation, we can write the thermopower S/T as [9–13]

$$\frac{S}{T} = -\frac{\pi^2 k_B^2}{3e}\left[\frac{\partial \ln \sigma(\varepsilon)}{\partial \varepsilon}\right]_{\varepsilon=\mu}, \tag{1}$$

where k_B and e are, respectively, the Boltzmann constant and the elementary charge, σ is the dc electric conductivity of the system, given by

$$\sigma(\varepsilon) = 2e^2\tau(\varepsilon)\int \delta(\mu-\varepsilon(\boldsymbol{p}))v(\boldsymbol{p})v(\boldsymbol{p})\frac{d\boldsymbol{p}}{(2\pi)^3}, \tag{2}$$

where $\boldsymbol{p}$ is the electron wave vector, τ is the scattering time, and v denotes the electron velocity. Thus, we see from Eq. (2) that the thermoelectric power S/T is sensitive to the derivative of the density of electronic states, $N(\varepsilon=\mu)$, and the change in the relaxation time at $\varepsilon=\mu$. On the basis of the Fermi liquid theory description, the term in the brackets on the right-hand side of Eq. (1) can be simplified, so that one has $S/T \propto N(\varepsilon=\mu) \propto C/T \propto M^*$ at $T \to 0$ [10–13]. As a result, upon taking into account that charge and heat currents at low temperatures are transported by quasiparticles, the ratio

$$(S/C) \simeq (S/S_{ent}) \simeq \text{constant}, \tag{3}$$

where S_{ent} is the entropy density of charge carriers [10–13]. Thus, we expect that within FC theory, one can obtain an adequate description of the thermopower and its scaling behavior, for the theory is based on the quasiparticle paradigm [3, 4, 14–16].

In FC theory, the QCP is interpreted as the fermion-condensation quantum phase transition (FCQPT) at which the quasiparticle effective mass M^* diverges. In such an event, quasiparticles of energy ε remain well-defined excitations near the chemical potential μ ($\varepsilon \sim \mu$) [3, 4] while the FC state itself is protected by topological

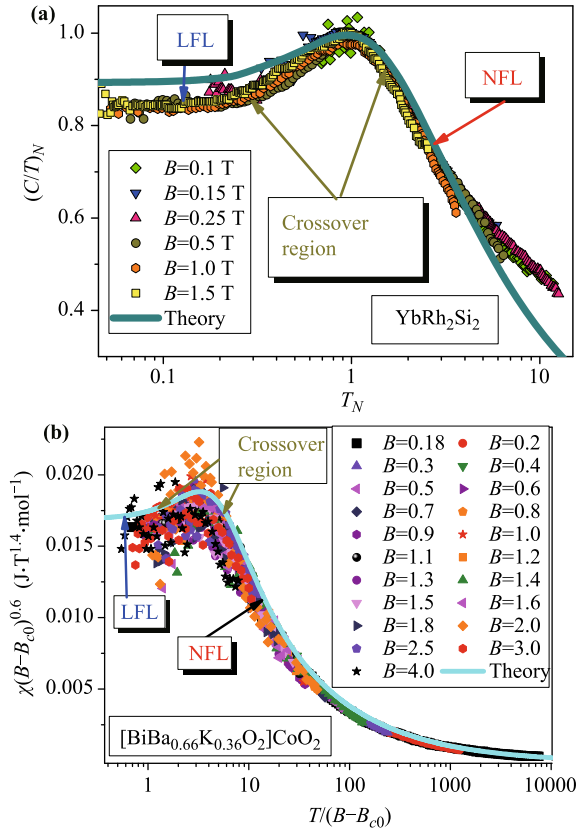

Fig. 1 The scaling behavior of the thermodynamic functions. **(a)** The normalized specific heat $(C/T)_N$ versus normalized temperature T_N. $(C/T)_N$ is extracted from the measurements of the specific heat C/T on $YbRh_2Si_2$ in magnetic fields B [5] listed in the legend. The LFL region, crossover one, and NFL one are depicted by the arrows. The solid curve displays calculations of $(C/T)_N = M_N^*$ based on Eqs. (4) and (5) [6]. **(b)** Scaled susceptibility $\chi(B-B_{c0})^{0.6}$ as a function of scaled temperature $T/(B-B_{c0})$ with $B_{c0} = 0.176$ T for various B values shown in the legend [20]. The LFL region, crossover one, and NFL one are shown by the arrows. The solid curve tracks the results of our calculations based on Eq. (4) that describe the universal scaling behavior $(C/T)_N = M_N^* \propto \chi(B-B_{c0})^{0.6}$ shown in Fig. 1(a).

invariants [17, 18]. In the vicinity of the FCQPT, it is helpful to use "internal" scales to measure such quantities as, e.g., C/T, M^*, and the temperature T to reveal the universal scaling behavior of M^* observed in HF compounds [3, 4]. Maximum structures $(C/T)_M \propto M^*_M$ in both C/T and M^*, respectively, at temperature T_M appear with the application of magnetic field B, and T_M acquires higher values as B is increased. To obtain $(C/T)_N$, we use $(C/T)_M$ and T_M as "internal" scales: $(C/T)_M$ is used to normalize C/T, and T is normalized by T_M [3, 4]. In the same way, we normalize M^* to obtain the normalized effective mass $M^*_N = M^*/M^*_M$ as a function of the normalized temperature $T_N = T/T_M$. To study the scaling behavior of $M^*(B,T)$, we use the model of a homogeneous HF liquid, which allows us to avoid complications associated with the crystalline anisotropy of solids, while the Landau equation describing $M^*(T,B)$ of an HF liquid reads [3, 4, 19]

$$\frac{1}{M^*(T,B)} = \frac{1}{M} + \int \frac{\boldsymbol{p}_F \boldsymbol{p}}{p_F^3} F(\boldsymbol{p}_F, \boldsymbol{p}) \frac{\partial n(T,B,\boldsymbol{p})}{\partial \boldsymbol{p}} \frac{\mathrm{d}\boldsymbol{p}}{(2\pi)^3}, \tag{4}$$

where M is the corresponding bare mass, $F(\boldsymbol{p}_F, \boldsymbol{p})$ is the Landau interaction, which depends on Fermi momentum p_F and momentum p, and n is the distribution function. Near the FCQPT, the normalized solution of Eq. (4), $M^*_N(T_N)$, can be well approximated by a simple universal interpolating function [3, 4]. The interpolation occurs between the LFL and NFL regimes and represents the universal scaling behavior of M^*_N:

$$M^*_N(y) \approx c_0 \frac{1 + c_1 y^2}{1 + c_2 y^{8/3}}. \tag{5}$$

Here, $y = T_N = T/T_M$, $c_0 = (1+c_2)/(1+c_1)$, and c_1 and c_2 are fitting parameters. The magnetic field B enters Eq. (4) only in the combination B/T, making $T_M \propto B$. Thus, in the presence of a fixed magnetic field the variable y becomes $y = T/T_M \sim T/B$. Thus, Eq. (5) describes the universal scaling behavior of M^*_N as a function of T versus B; the curves M^*_N at different magnetic fields B merge into a single one in terms of the normalized variable $y = T/T_M$. In the same way, Eq. (5) describes the scaling behavior of $M^*_N(B,T)$ as a function of B versus T [3, 4, 6, 19].

Figure 1(a) shows the resulting $(C/T)_N$ as a function of T_N, with different symbols for different magnetic field strengths B. The solid curve represents calculations of $(C/T)_N = M^*_N$ based on Eqs. (4) and (5) [6]. It is seen that the LFL and NFL regions are separated by a crossover region where $(C/T)_N$ reaches its maximal value. As evident from Fig. 1(a), $(C/T)_N$ is not a constant, as would be the case for an LFL; furthermore, the figure demonstrates the asserted universal scaling behavior given by Eq. (5) over a wide range of values of the normalized temperature T_N. This behavior coincides with that of the magnetic susceptibility $\chi \propto C/T \propto M^*$ revealed in measurements on $[BiBa_{0.66}K_{0.36}O_2]CoO_2$ [20] and incorporated in Fig. 1(b). The solid curve tracks the results of the same calculations based on Eq. (4) that describe the universal scaling behavior $(C/T)_N(T/T_M) = M^*_N(T/T_M) \propto \chi(B-B_{c0})^{0.6}$ shown in Fig. 1(a). We thus conclude that the solid curve drawn in Figs. 1(a) and 1(b) exhibits the universal scaling behavior intrinsic to HF compounds [3, 4]. It is seen from Fig. 2 that, in the case of $YbRh_2Si_2$ and at $T \geqslant T_{NL}$, the isotherms $-S(B)/T$ behave like C/T: They exhibit a broad maximum that sharpens and shifts to lower fields upon cooling [21, 22]. It is seen from Fig. 2 that the mentioned behavior is violated as the system approaches the AF phase transition taking place at $T_{NL}(B)$. Here $T_{NL}(B)$ is the temperature of AF ordering, with $T_{NL}(B=0) = 70$ mK, and $T_{NL}(B = B_{c0}) = 0$ at the critical field $B_{c0} = 60$ mT, applied perpendicular to the magnetically hard c axis [23]. Thus, we can expect that, outside the AF region, $S/T \propto C/T \propto \chi \propto M^*$ over a wide range of T and B, since in the framework of FC theory quasiparticles are responsible for the thermodynamic and transport properties [3, 4]. It is worth noting that $S/T \propto M^*$ in a low-disorder two-dimensional electron system in silicon and tends to diverge at a finite disorder-independent density [24].

To reveal the scaling behavior of the thermopower $S/T \propto C/T \propto M^*$, we normalize S/T in the same way as in the normalization of C/T: The normalized function $(S/T)_N$ is obtained by normalizing (S/T) by its maximum value, occurring at $T = T_M$, and the temperature

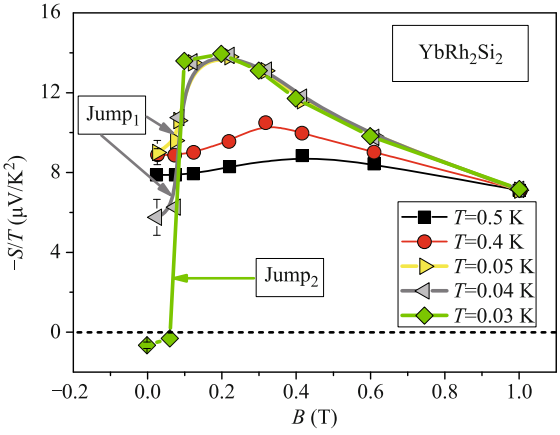

Fig. 2 Thermopower isotherm $-S(B)/T$ for different temperatures shown in the legend [21, 22]. The labels Jump_1 and Jump_2 represent the first and second downward jumps in $-S(B)/T$ shown by the arrows. The solid lines are guides to the eye.

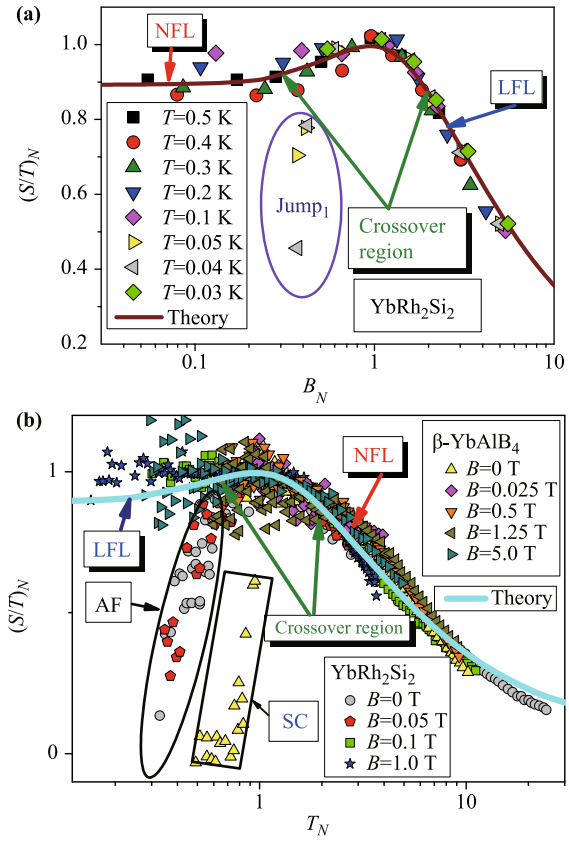

Fig. 3 Scaling behavior of S/T. **(a)** Normalized isotherm $(S(B)/T)_N$ versus normalized magnetic field B_N for different temperatures shown in the legend. Outside the AF phase transition, the data follow the universal scaling curve shown in Fig. 1(a). **(b)** Temperature dependence of the normalized thermopower $(S/T)_N$ under several magnetic fields shown in the legend. The experimental data are extracted from measurements on $YbRh_2Si_2$ [21, 22] and on β-$YbAlB_4$ [25]. As it is explained in the text, the data, taken at the AF phase [21, 22] and at the superconducting one (SC) [25] and confined by both the ellipse and the rectangle, respectively, signal of violation of the scaling behavior. The solid curves in (a) and (b) represent calculated $(C/T)_N$ displayed in Fig. 1(a) [6].

T is scaled by T_M. Taking into account that $S/T \propto C/T$ [11–13], we conclude that $(S/T)_N = (C/T)_N = M_N^*$, provided that the system in question is located away from possible phase transitions. This function $(C/T)_N = M_N^*$ is displayed in Fig. 1(a). Figures 3(a) and 3(b) report $(S/T)_N$ as a function of the normalized magnetic field B_N and T_N, respectively. In Fig. 3(a), the function $(S/T)_N$ is obtained by normalizing (S/T) by its maximum occurring at B_M, and the field B is scaled by B_M. As seen from Eq. (5), the LFL behavior takes place at $B_N > 1$, since $(S/T)_N = M_N^*$, and $M_N^* \propto (B - B_{c0})^{-2/3}$ is T-independent, while at $B_N < 1$, M_M^* becomes T-dependent and exhibits the NFL behavior with $M_N^* \propto T_N^{-2/3}$. It is seen from Figs. 3(a) and 3(b) that the calculated values of the universal function M_N^* are in good agreement with the corresponding experimental data over the wide range of the normalized magnetic field. Thus, $(S/T)_N = (C/T)_N = M_N^*$ exhibits the universal scaling behavior over a wide range of its scaled variable B_N and T_N. Figure 3(a) also depicts a violation of the scaling behavior for $B \leqslant B_{c0}$ when the system enters the AF phase. Moreover, as seen from Figs. 2 and 3(a) and 3(b), the scaling behavior is violated at $T \leqslant T_{NL}$ by two downward jumps. The first jump, shown in Figs. 2 and 3(a) and labeled Jump_1, takes place at $T_{NL} > T > 0.3$ K, while the second, occurring at $T \leqslant 0.03$ K, is shown in Fig. 2 and is labeled Jump_2. The latter is accompanied by a change of sign of $(S/T)_N$, which now becomes positive [21, 22]. As we shall see, these two jumps reflect the presence of a flat band at μ in the single-particle spectrum $\varepsilon(\boldsymbol{p})$ of heavy electrons in $YbRh_2Si_2$ [3, 4]. In the same way, as is seen from Fig. 3(b), the scaling behavior is violated by the superconducting (SC) phase transition, taking place in β-$YbAlB_4$ at $T_c \simeq 80$ mK [25].

We now further show that the observed scaling behavior of $(S/T)_N$ is universal by analyzing the experimental data on the thermopower for $[BiBa_{0.66}K_{0.36}O_2]CoO_2$ [20]. The solid curve, representing our calculations in Fig. 4, is the same as that depicted in Fig. 1(a) and describes $(C/T)_N$ extracted from measurements on the archetypal HF metal $YbRh_2Si_2$ [6]. By plotting $(S/T)_N$ as a function of T_N in Fig. 4, the universal scaling behavior and the three regimes are seen to be in complete agreement with the reported overall behavior in Figs. 1(a) and Figs. 3(a) and 3(b) as well. Our preliminary results show that Ce-based HF compounds such as $CeCoIn_5$ exhibit the same scaling behavior of $(S/T)_N$ and will be published elsewhere.

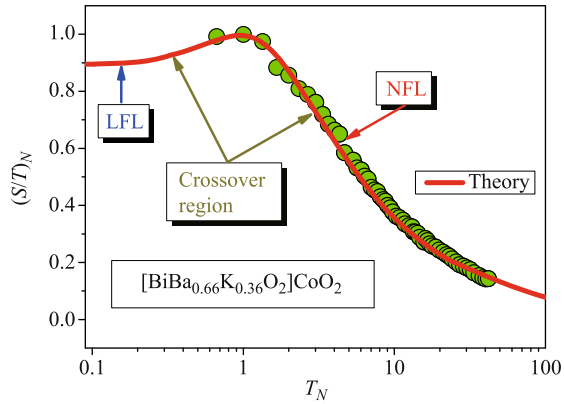

Fig. 4 Scaling behavior of S/T in the strongly correlated layered cobalt oxide $[BiBa_{0.66}K_{0.36}O_2]CoO_2$. Temperature dependence of $(S(T)/T)_N$ at magnetic field $B = 0$, extracted from measurements on $[BiBa_{0.66}K_{0.36}O_2]CoO_2$ [20], is displayed versus T_N. The solid curve representing the theoretical calculations is the same as that depicted in Fig. 1(a).

3 Flat bands and the jumps in S/T at the AF phase transition

Before proceeding to the analysis of the jumps observed in measurements of S/T on $YbRh_2Si_2$, some remarks are in order concerning the flattening of the spectra $\varepsilon(\boldsymbol{p})$ in HF systems, a phenomenon called swelling of the Fermi surface or FC [3, 4, 14]. As indicated in Fig. 5, the ground states of systems with flat bands are degenerate, and therefore the occupation numbers $n_0(\boldsymbol{p})$ of single-particle states belonging to a flat band are given by a continuous function on the interval $[0, 1]$, in contrast to the FL restriction to occupation numbers 0 and 1. This property leads to an entropy excess

$$S_0 = -\sum n_0(\boldsymbol{p}) \ln n_0(\boldsymbol{p}) + (1 - n_0(\boldsymbol{p})) \ln(1 - n_0(\boldsymbol{p})), \tag{6}$$

which does not contribute to the specific heat $C(T)$. The entropy excess S_0 contradicts the Nernst theorem. To circumvent violation of the Nernst theorem, FC must be completely eliminated at $T \to 0$. This can occur by virtue of some phase transition, e.g., the AF transition that becomes of first order at some tricritical point occurring at $T = T_{\rm tr}$ [3, 4]. Such a first-order phase transition eliminates the flat portion in the spectrum $\varepsilon(\boldsymbol{p})$. As a consequence, both the density of states, N, and the hole states, shown by the arrow in Fig. 5, vanish discontinuously, while the occupation numbers $n_0(\boldsymbol{p})$ and the spectrum $\varepsilon(\boldsymbol{p})$ revert to those LFL state values, as indicated by the arrows in Fig. 3(a). Simultaneously, the Fermi sphere undergoes an abrupt change on the interval from the Fermi momentum p_f to p_F, so as to nullify both the swelling of the Fermi surface and the entropy

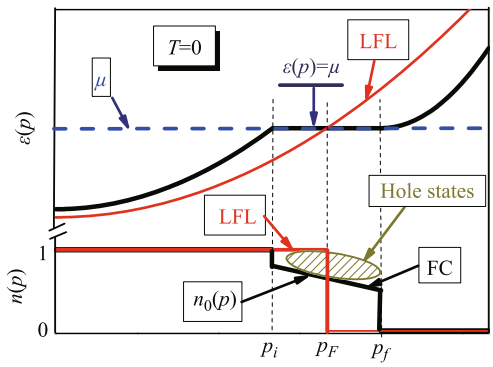

Fig. 5 Single-particle energy $\varepsilon(\boldsymbol{p})$ and distribution function $n(\boldsymbol{p})$ at $T = 0$. The arrow shows the chemical potential μ. The vertical lines show the area $p_i < p < p_f$ occupied by FC with $0 < n_0(p) < 1$ and $\varepsilon(\boldsymbol{p}) = \mu$. The Fermi momentum p_F satisfies the condition $p_i < p_F < p_f$ and corresponds to the LFL region, indicated by the arrows, that emerges when the FC state is eliminated. The arrow depicts hole states induced by the FC.

excess S_0. As a result, the thermopower experiences Jump_2, as follows from Eq. (3), for the entropy abruptly diminishes. We note that the abrupt change is observed as the change of the low-T Hall coefficient [3, 4, 23, 26]. It is seen from Fig. 2 that, at $T = 0.03$ K, S/T abruptly changes its sign (the second jump, Jump_2), for the hole states vanish. The positive sign of S/T of $YbRh_2Si_2$ without the hole states [12] is in agreement with the positive thermopower of its nonmagnetic counterpart $LuRh_2Si_2$, lacking the $4f$ hole states at μ [21, 22, 27]. In contrast, at $T_{NL} > T > T_{cr}$, the AF phase transition is of second order and the entropy is a continuous function at the border of the phase transition. Therefore, at this second-order phase transition neither the occupation numbers nor the spectrum change, and the spectrum keeps its FC-like shape, while the system with FC is destroyed, being converted into an HF liquid. This destruction generates the first jump, Jump_1, shown in Fig. 2. Therefore, as the FC state decays, its contribution ρ_0^{FC} to the residual resistivity ρ_0 vanishes, resulting in a change of the scattering time $\tau(\varepsilon = \mu)$. We recall that, in the presence of FC, the residual resistivity consists of two terms, $\rho_0 = \rho_0^{FC} + \rho_0^{imp}$, where the residual resistivity ρ_0^{FC} is formed by the flat band generated by FC, while the resistivity ρ_0^{imp} is formed by impurities [4, 28, 29]. As a result, the thermopower experiences the first jump Jump_1, as seen from Eqs. (1) and (2). We also conclude that the second downward jump under decreasing B is deeper than the first one, since it is caused by elimination of both ρ_0^{FC} and the hole states. This is consistent with the experimental observations, as seen from Fig. 2.

4 Schematic T–B phase diagram

Now we are in position to construct the T–B phase diagram of the archetypal HF metal $YbRh_2Si_2$. Figure 6 displays our constructed schematic T–B phase diagram for $YbRh_2Si_2$. In Fig. 6, the NFL region, formed by the FC state, is characterized by the entropy excess S_0 given by Eq. (6) and is labeled by FC. As shown by the solid curve denoted by $T_{NL}(B)$, at $B < B_{c0}$ and $T < T_{NL}(B)$ the system is in its AF state, and it exhibits LFL behavior [23]. The tricritical point $T_{\rm cr}$ at which the AF phase transition becomes of first order is indicated by the arrow. At that transition the thermopower experiences the jump Jump_2 shown in Fig. 2 and changes its sign, becoming $S/T > 0$, for the hole states shown in Fig. 5 vanish at $T < T_{\rm cr}$. At $T > T_{\rm cr}$ the AF transition is of second order, and at this transition the thermopower experiences Jump_1 (see Fig. 2), while in the NFL region $S/T > 0$, as is shown in the phase diagram of Fig. 6. Clearly, on

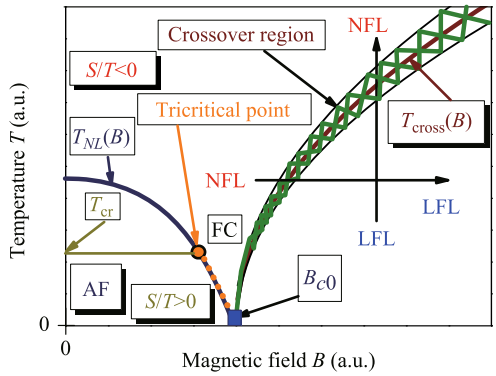

Fig. 6 Schematic T–B phase diagram of $YbRh_2Si_2$. The vertical and horizontal arrows, crossing the transition region depicted by the thick lines, show the LFL-NFL and NFL-LFL transitions at fixed B and T, respectively. The hatched area around the solid curve $T_{\rm cross}(B)$ represents the crossover between the NFL and LFL domains. The NFL region is labeled by FC. As shown by the solid curve, at $B < B_{c0}$ the system is in its AF state, and exhibits the LFL behavior [23]. The line of AF phase transitions is denoted by $T_{NL}(B)$. The tricritical point, indicated by the arrow, is at $T = T_{\rm cr}$. At $T < T_{\rm cr}$ the AF phase transition becomes of the first order.

the basis of the phase diagram of Fig. 6, outside the area of the AF phase transition, the behavior of $S_N = M_N^*$, considered as a function of the dimensionless variable T_N or B_N, is almost universal. Indeed, as seen from Figs. 1(a), 1(b), 3(a), 3(b), and 4, all the data extracted from measurements on $YbRh_2Si_2$, β-$YbAlB_4$, and $[BiBa_{0.66}K_{0.36}O_2]CoO_2$ collapse onto the single scaling curve shown in Fig. 1(a). As seen from Figs. 1(a) and 3(b), at $T_N < 1$, $(S/T)_N$ tends to become constant, implying that S/T exhibits LFL behavior. However, at $T_N \simeq 1$ the system enters the narrow crossover region, while at growing temperatures, NFL behavior prevails.

5 Conclusions

In summary, we have revealed and explained the universal scaling behavior of the thermopower S/T in different HF compounds such as $YbRh_2Si_2$, β-$YbAlB_4$, and $[BiBa_{0.66}K_{0.36}O_2]CoO_2$. Our calculations are in good agreement with experimental observations and demonstrate that the advocated universal scaling behavior of S/T does take place. This behavior does not depend on the specific properties of the considered HF compounds, and it coincides with that of the normalized effective mass $M_N^* = (C/T)_N$, thus representing the scaling behavior intrinsic to HF compounds. We have also shown that destruction of the flattening of the single-particle spectrum profoundly affects S/T, leading to the two jumps and the change of sign of the thermopower occurring at the AF phase transition.

Acknowledgements V. R. S. thanks the RSF Grant, # 14-22-00281. A. Z. M. thanks the US DOE, Division of Chemical Sciences, Office of Energy Research, and ARO for research support. K. G. P. was supported by Grant No. 11.38.658.2013 and RFBR No. 14-02-00044. V. A. K. and J. W. C. acknowledge research support from the McDonnell Center for the Space Sciences, and J. W. C. thanks the University of Madeira gracious hospitality during frequent visits.

References

1. P. Coleman, C. Pèpin, Q. Si, and R. Ramazashvili, How do Fermi liquids get heavy and die? *J. Phys.: Condens. Matter* 13(35), R723 (2001)
2. H. Löhneysen, A. Rosch, M. Vojta, and P. Wölfle, Fermi-liquid instabilities at magnetic quantum phase transitions, *Rev. Mod. Phys.* 79(3), 1015 (2007)
3. V. R. Shaginyan, M. Ya. Amusia, A. Z. Msezane, and K. G. Popov, Scaling behavior of heavy fermion metals, *Phys. Rep.* 492(2–3), 31 (2010)
4. M. Ya. Amusia, K. G. Popov, V. R. Shaginyan, and W. A. Stephanowich, Theory of Heavy-Fermion Compounds - Theory of Strongly Correlated Fermi-Systems, Springer-Verlag, 2015
5. N. Oeschler, S. Hartmann, A. Pikul, C. Krellner, C. Geibel, and F. Steglich, Low-temperature specific heat of $YbRh_2Si_2$, *Physica B* 403(5–9), 1254 (2008)
6. V. R. Shaginyan, M. Ya. Amusia, and K. G. Popov, Strongly correlated Fermi-systems: Non-Fermi liquid behavior, quasiparticle effective mass and their interplay, *Phys. Lett. A* 373(26), 2281 (2009)
7. K. S. Kim and C. Pépin, Thermopower as a signature of quantum criticality in heavy fermions, *Phys. Rev. B* 81(20), 205108 (2010)
8. K. S. Kim and C. Pépin, Thermopower as a fingerprint of the Kondo breakdown quantum critical point, *Phys. Rev. B* 83(7), 073104 (2011)
9. A. A. Abrikosov, Fundamentals of the Theory of Metals, Amsterdam: North-Holland, 1988
10. E. M. Lifshitz, L. D. Landau, and L. P. Pitaevskii, Electrodynamics of Continuous Media, New York: Elsevier, 1984
11. K. Behnia, D. Jaccard, and J. Flouquet, On the thermoelectricity of correlated electrons in the zero-temperature limit, *J. Phys.: Condens. Matter* 16(28), 5187 (2004)
12. K. Miyake and H. Kohno, Theory of quasi-universal ratio of seebeck coefficient to specific heat in zero-temperature limit in correlated metals, *J. Phys. Soc. Jpn.* 74(1), 254 (2005)
13. V. Zlatić, R. Monnier, J. K. Freericks, and K. W. Becker, Relationship between the thermopower and entropy of strongly correlated electron systems, *Phys. Rev. B* 76(8), 085122(2007)
14. V. A. Khodel and V. R. Shaginyan, Superfluidity in system with fermion condensate, *JETP Lett.* 51(9), 553 (1990)
15. P. Nozières, Properties of Fermi liquids with a finite range interaction, *J. Phys. I France* 2(4), 443 (1992)

16. V. A. Khodel, V. R. Shaginyan, and V. V. Khodel, New approach in the microscopic Fermi systems theory, *Phys. Rep.* 249(1–2), 1 (1994)
17. G. E. Volovik, A new class of normal Fermi liquids, *JETP Lett.* 53(4), 222 (1991)
18. G. E. Volovik, From Standard Model of particle physics to room-temperature superconductivity, *Phys. Scr.* T164, 014014 (2015)
19. L. D. Landau, Theory of Fermi liquid, *Sov. Phys. JETP* 30(6), 920 (1956)
20. P. Limelette, W. Saulquin, H. Muguerra, and D. Grebille, From quantum criticality to enhanced thermopower in strongly correlated layered cobalt oxide, *Phys. Rev. B* 81(11), 115113 (2010)
21. S. Hartmann, N. Oeschler, C. Krellner, C. Geibel, S. Paschen, and F. Steglich, Thermopower evidence for an abrupt Fermi surface change at the quantum critical point of $YbRh_2Si_2$, *Phys. Rev. Lett.* 104(9), 096401 (2010)
22. S. Friedemann, S. Wirth, S. Kirchner, Q. Si, S. Hartmann, C. Krellner, C. Geibel, T. Westerkamp, M. Brando, and F Steglich, Break up of heavy fermions at an antiferromagnetic instability, *J. Phys. Soc. Jpn.* 80(10), SA002 (2011)
23. P. Gegenwart, J. Custers, C. Geibel, K. Neumaier, T. Tayama, K. Tenya, O. Trovarelli, and F. Steglich, Magnetic-field induced quantum critical point in $YbRh_2Si_2$, *Phys. Rev. Lett.* 89(5), 056402 (2002)
24. A. Mokashi, S. Li, B. Wen, S. V. Kravchenko, A. A. Shashkin, V. T. Dolgopolov, and M. P. Sarachik, Critical behavior of a strongly interacting 2D electron system, *Phys. Rev. Lett.* 109(9), 096405 (2012)
25. Y. Machida, K. Tomokuni, C. Ogura, K. Izawa, K. Kuga, S. Nakatsuji, G. Lapertot, G. Knebel, J. P. Brison, and J. Flouquet, Thermoelectric response near a quantum critical point of $YbAlB_4$ and $YbRh_2Si_2$: A comparative study, *Phys. Rev. Lett.* 109(15), 156405 (2012)
26. S. Paschen, T. Lühmann, S. Wirth, P. Gegenwart, O. Trovarelli, C. Geibel, F. Steglich, P. Coleman, and Q. Si, Hall-effect evolution across a heavy-fermion quantum critical point, *Nature* 432(7019), 881 (2004)
27. U. Köhler, N. Oeschler, F. Steglich, S. Maquilon, and Z. Fisk, Energy scales of $Lu_{1-x}Yb_xRh_2Si_2$ by means of thermopower investigations, *Phys. Rev. B* 77(10), 104412 (2008)
28. V. R. Shaginyan, A. Z. Msezane, K. G. Popov, J. W. Clark, M. V. Zverev, and V. A. Khodel, Magnetic field dependence of the residual resistivity of the heavy-fermion metal $CeCoIn_5$, *Phys. Rev. B* 86(8), 085147 (2012)
29. V. R. Shaginyan, A. Z. Msezane, K. G. Popov, J. W. Clark, M. V. Zverev, and V. A. Khodel, Nature of the quantum critical point as disclosed by extraordinary behavior of magnetotransport and the Lorentz number in the heavy-fermion metal $YbRh_2Si_2$, *JETP Lett.* 96(6), 397 (2012)